

Effect of Mean Flow on the Transmission Loss of a Doubly Tuned Flow Reversal Muffler

Chetan Dayanand Gaonkar^{1,*}, Thappaganadoddi Nagabushnasharma Sreenivasa²

¹Department of Mechanical Engineering, VTU Belagavi, Karnataka, India/Department of Mechanical Engineering, Don Bosco College of Engineering, Goa, India

²Department of Mechanical Engineering, VTU Belagavi, Karnataka, India

Received 23 April 2024; received in revised form 23 May 2024; accepted 24 May 2024

DOI: <https://doi.org/10.46604/aiti.2024.13620>

Abstract

The same-end-inlet-outlet (SEIO) muffler, also referred to as a flow reversal muffler under flow conditions, features inlet and outlet pipes positioned on the same side of the chamber. Recently, a parametric expression has been developed to determine the end correction for double tuning of the SEIO muffler. This study extends the development of the SEIO muffler by experimentally validating the derived end correction expressions. Additionally, the tuning of the muffler is assessed with a mean flow using 3-D computational fluid dynamics, solving the linearized Navier-Stokes equation. This investigation explores the impact of flow conditions (Mach number 0.05 and 0.1) and temperature conditions ($T = 733$ K and 953 K) on the transmission loss (TL) of a doubly tuned muffler. The findings reveal that the muffler maintains its double tuning, even in the presence of mean flow at elevated temperatures, albeit with somewhat of a reduction in performance.

Keywords: transmission loss, double tuning, flow reversal muffler, CFD, Mach number

1. Introduction

Fundamentally, an ideal exhaust muffler would have high insertion loss (IL)/transmission loss (TL), low back pressure, smaller size, spark arresting capability, minimum break-out noise, sufficiently low flow-generated noise within the muffler element and at the tailpipe, etc. Given the attributes stated above, researchers have been developing the mufflers using multifarious computational models, right from 1-D plane wave theory, transfer matrix method (TMM), and integrated transfer matrix (ITM) method to state-of-the-art techniques such as 3-D finite element method (FEM) and computational fluid dynamics (CFD) analysis. Development of the muffler commenced with a simple expansion chamber (SEC), whose TL is characterized by periodic domes and sharp troughs occurring at the integral multiples of π . Such a trough results in a sharp drop in the overall IL of the muffler [1].

To overcome the dramatic abatement in the overall IL, a doubly tuned extended tube chamber muffler was developed, which is superior in tuning out the first three of the four troughs of the TL curve, thereby yielding wide band TL as well as IL by deploying the 1-D plane wave analysis and the 3-D finite element analysis of the muffler [2-4]. Along these similar lines, recently, a same-end-inlet-outlet (SEIO) muffler was developed (refer to Fig. 1) by Gaonkar et al. [5]. Specifically, the double tuning of this muffler (refer to Fig. 2) was ideally managed using TL expression, as shown in the formula below and the FEM technique.

* Corresponding author. E-mail address: chetan.gaonkar@dbcegoa.ac.in

$$TL = 20 \log \left[\left(\frac{Y_1}{Y_n} \right)^{1/2} \left| \frac{T_{11} + T_{12}/Y_1 + Y_n T_{21} + (Y_n/Y_1) T_{22}}{2} \right| \right] \quad (1)$$

where, $Y = c_0/A$ denotes characteristics impedance. Suffixes 1 and n denotes 1st and n^{th} element of the muffler respectively, while C_0 is the speed of sound and A is the cross-sectional area of inlet and outlet exhaust pipes. T_{11} , T_{12} , T_{21} , and T_{22} are the four pole parameters [1], which are functions of impedances, resonator lengths, and excitation frequency.

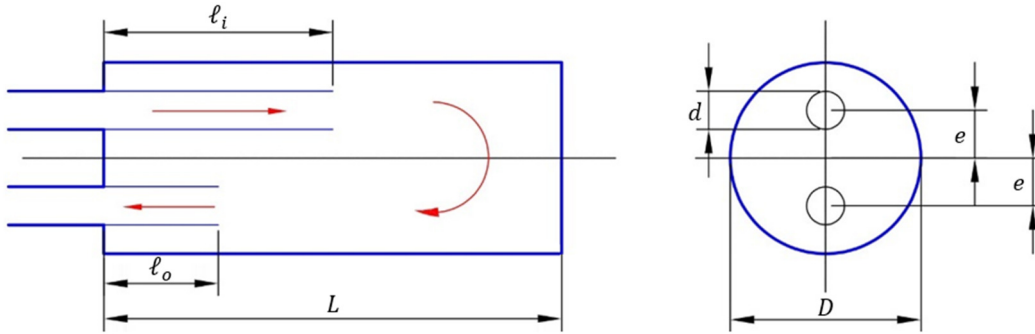


Fig. 1 Schematic of same-end-inlet-outlet (SEIO) muffler

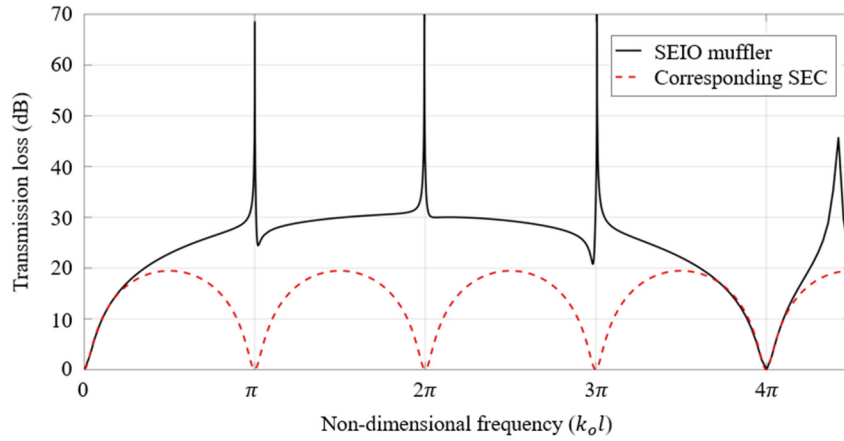


Fig. 2 TL plot of SEIO vs corresponding SEC muffler

Meanwhile, the parametric expression, as shown in the formula below, emerged to determine the end corrections δ_i and δ_o at the inlet and outlet pipe respectively (refer to Table 1 for parameters).

$$\frac{\delta_i}{d} = 0.4668 - 1.8631 \left(\frac{d}{D} \right) + 4.228 \left(\frac{d}{D} \right)^2 + 0.9149 \left(\frac{t_w}{d} \right) - 0.3575 \left(\frac{e}{D} \right) + 1.2904 \left(\frac{e}{D} \right)^2 \quad (2)$$

$$\frac{\delta_o}{d} = 0.4042 - 1.0333 \left(\frac{d}{D} \right) + 2.6457 \left(\frac{d}{D} \right)^2 + 0.8718 \left(\frac{t_w}{d} \right) - 0.6925 \left(\frac{e}{D} \right) + 1.7998 \left(\frac{e}{D} \right)^2 \quad (3)$$

However, these derived expressions were not verified against the experimental measurements. Hence, the first objective of this work is to experimentally validate these derived expressions.

Table 1 Parameters of muffler for – with and without end correction (dimensions in mm)

Parameter	Without end correction	With end correction
Diameter of chamber (D)	130	130
Length of chamber (L)	520	520
Diameter of inlet and outlet pipe (d)	30	30
Length of inlet pipe (ℓ_i)	260	251
Length of outlet pipe (ℓ_o)	30	121
The wall thickness of inlet and outlet pipe (t_w)	1.6	1.6
Eccentricity (e)	32	32

The study of flow reversal mufflers commenced approximately half a century ago when Young and Crocker [6] established a theoretical model and used FEM to predict the TL of this muffler. As a result, mathematical equations were established using analytical approaches to predict the TL in the chambers [7-8], and the influence of end correction was studied using a semi-analytical approach [9]. The formulation of end-correction expressions apropos muffler geometric characteristics, has been a recent advancement in the flow reversal muffler [5]. All of these preceding studies, however, have been conducted in the absence of mean flow, i.e., for stationary medium. The first attempt to study the effect of flow in these flow-reversal mufflers was by Panicker and Munjal [10] where the transfer matrices pertinent to the aeroacoustics variables across flow-reversing elements were derived. Broatch et al. [11] incorporated the CFD simulation to compute the acoustic response while accounting for nonlinear dissipation and solving the full Navier-Stokes equation in the time domain.

Recently, a few researchers employed the strategy of incorporating CFD simulation and have attested to the use of steady computational results on acoustic mesh and further solve frequency domain acoustic problems using a systematic mapping technique [12-13]. Liu et al. [14] presented a time-domain simulation method to predict the IL of a dissipative muffler with exhaust flow, which is a key acoustic index for muffler design. He et al. [15] used a two-step numerical approach using steady-state CFD and linearized Navier-Stokes equations (LNSEs) to solve for acoustic perturbation variables. The comparisons between numerical predictions and experimental measurements exhibit decent consistency. Subsequently, the LNSE was used to compute the acoustic performance of the perforated mufflers in the case of non-uniform flow. Furthermore, the result achieved an ideal agreement with the experimental measurements [16].

Mohamad et al. [17] used CFD to ascertain the effect of perforated tube configurations on the performance of exhaust mufflers with mean flow, focusing on the real walls approach with a surface roughness of 0.5 micrometers. Moreover, recently, the modified TMM (MTMM) combining 3D-CFD with the classic TMM has been introduced to predict the TL of automotive exhaust mufflers [18]. In the presence of the mean flow, convective and dissipative effects will emerge on the acoustic field, which may further influence the overall TL curve of the muffler. The previous discussion clearly shows that using CFD for mean flow simulation to predict the acoustic properties of mufflers (such as TL) is becoming increasingly popular due to its accuracy and cost-effectiveness compared to multiple experimental measurements.

However, no attempt has been made to understand the effect of mean flow, on the double tuning of any muffler. Hence, the second objective of this work is to ascertain the effect of mean flow on the double tuning of a flow reversal muffler using a comprehensive CFD solution approach. The influence of flow and temperature on the TL curve will be investigated in this study, confirming whether the muffler can retain its double tuning in the presence of flow at higher Mach numbers and temperatures.

Following this introduction, Section 2 briefly describes the experimental technique used to validate the end correction expression. Section 3 discusses in detail, the CFD simulation to predict the TL. Computational results are presented in Section 4, and concluding remarks in Section 5.

2. Experimental Validation

As discussed in the preceding section, to validate the end correction expressions, two mufflers, i.e., one with and one without end corrections are fabricated. The muffler without end corrections can be termed as an untuned muffler, and likewise, the muffler with end corrections can be termed as a tuned muffler. The specifications of the two mufflers under consideration are listed below in Table 1 (refer to Fig. 1 for the parameters).

To double tune the muffler using extended inlet and outlet exhaust pipes, the length of the inlet pipe should be $l_i = L/2 = 520/2 = 260$ mm, and that of the outlet pipe should be $l_o = L/4 = 520/4 = 130$ mm. Furthermore, Eqs. (2)-(3) are used to calculate the end corrections for the inlet and outlet pipes with the parameters, as shown in Table 1, which yields $\delta_i = 9.2754$

mm and $\delta_o = 9.0452$ mm. According to the theory of end corrections, the values require to be subtracted from the geometric lengths (l_i, l_o) to tune the muffler [1]. Hence, the new pipe lengths of the tuned muffler configuration are presented as follows:

- Inlet pipe = $l_i - \delta_i = 260 - 9.2754 = 250.7246$ mm ≈ 251 mm (for fabrication purposes)
- Outlet pipe = $l_o - \delta_o = 130 - 9.0452 = 120.9548$ mm ≈ 121 mm (for fabrication purposes)

The effect of these rounded-off lengths for fabrication will be minimal (negligible) on the measured TL values.

The TL of the SEIO muffler was measured using the two-load method. Rather than changing the sources, the end load is altered to produce two configurations. Two types of end loads are used herein: anechoic termination and reflected termination. These two configurations, like the two-source technique, yield four equations, which are then used to calculate the four-pole parameter and consequently the TL of the muffler.

Test equipment used are:

- (1) Multi-channel data acquisition system PULSE, Type 3560-B-130, B & K Denmark make
- (2) Power Amplifier, Type UBA-500, Ahuja make
- (3) Muffler Test Rig with Sound Source, ARAI make
- (4) Half-inch condenser microphones, P.C.B. make

The test was performed under no mean flow condition with a lower cut-off frequency of 40 Hz and at an ambient temperature of 25 °C. The experimental setup is shown in Fig. 3. The loudspeaker was used as a source of excitation, producing a random noise signal.

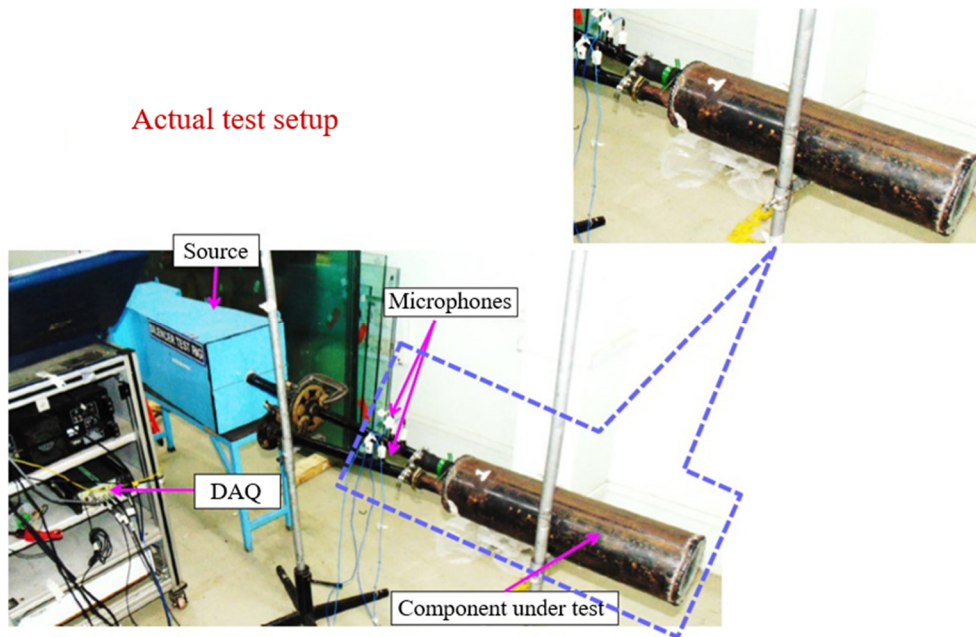


Fig. 3 Experimental setup of TL measurement of SEIO muffler

The TL plots generated from experimental measurements are depicted in Fig. 4 and Fig. 5 for an untuned and tuned muffler, respectively. The frequency resolution used for the TL measurement was 8 Hz, resulting in a less precise representation of sharp peaks. Notwithstanding the limitations in capturing sharp peaks, the experimental results align with the trend, which is observed in the TL plot obtained through 3-D FEM. Hence, it validates the expressions derived (Eqs. (1)-(2)) to predict the end correction in a SEIO muffler. However, fabrication flaws, e.g., deviations from the prescribed lengths and eccentricity of the inlet and outlet exhaust pipes, could be a possible explanation for the slight variation in the 2nd and 3rd peaks between the predicted and measured TL plots (see Fig. 5).

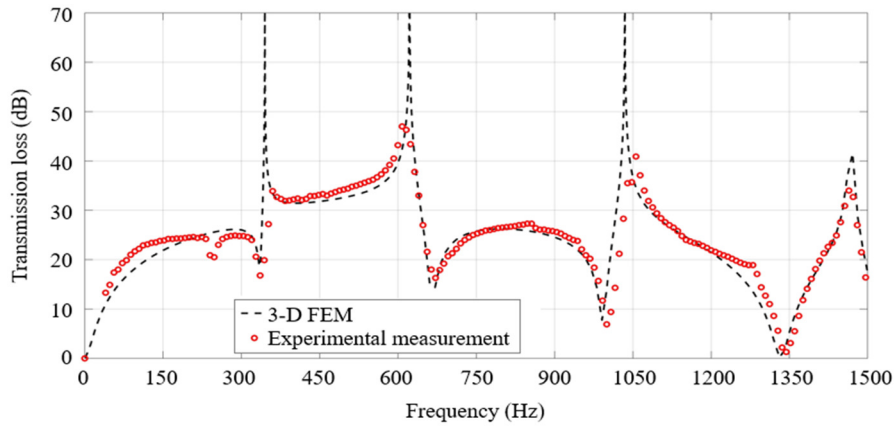


Fig. 4 Measured TL plot of an untuned muffler

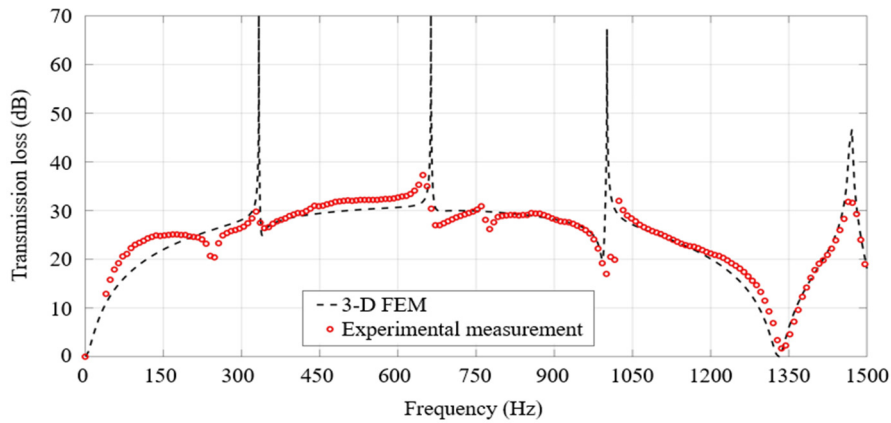


Fig. 5 Measured TL plot of the tuned muffler

3. CFD Analysis to Predict the TL

The TL of the muffler is influenced by the presence of flow in the exhaust system, which in turn alters the acoustic properties of the system. As discussed in the introduction, the influence of mean flow on the acoustic field of the muffler has been evaluated both theoretically and computationally. However, the use of computational methods, including CFD analysis, to predict the TL of a muffler gradually gains utilization.

3.1. Theory

When the flow (hot exhaust gases) of uniform velocity U inside the system is present, the forward sound wave moves at an absolute velocity of $U + C_o$ and the backward sound wave at $U - C_o$, where C_o is the speed of sound. Thus, the general solution to a 1-D wave equation as below for a cylindrical duct concerning pressure p and velocity v as a function of coordinate z and time t becomes:

$$p(z,t) = \left(C_1 e^{-jk_o z/1+M} + C_2 e^{+jk_o z/1-M} \right) e^{j\omega t} \tag{4}$$

$$v(z,t) = \frac{1}{Y_o} \left(C_1 e^{-jk_o z/1+M} + C_2 e^{+jk_o z/1-M} \right) e^{j\omega t} \tag{5}$$

where C_1 and C_2 are the constants to be determined using boundary conditions, $M = u_o/c_o$ is the Mach number, $k_o = \omega/c_o$ is the wave number, $\omega = 2\pi f$ is the radian frequency, and f is the excitation frequency.

Using this solution one can compute the acoustic energy flux and thence the TL. Moreover, deploying the TMM (Eq. (1)) and incorporating the Mach number in the expression one can compute the TL of the muffler in the presence of mean flow. Despite the effectiveness of the estimation of TL using these methods, results deviate from the experimental results in the case

of complex mufflers [19]. The muffler considered in this work yields a bias and reversal flow, and the acoustic field therein is clearly three-dimensional, therefore demands more sophisticated 3-D CFD analysis to predict the TL in the presence of the fluid flow.

The turbulent flow presented within the muffler’s flow field can be analyzed using the LNSEs [20]. These equations represent a simplified version of the classical Navier-Stokes equations and serve as a linearization of the governing equations for compressible, viscous, and nonisothermal flows. The governing equations are the continuity, momentum, and energy equations:

$$\frac{\partial \rho_t}{\partial t} + \nabla \cdot (\rho_o u_t + \rho_t u_o) = M \tag{6}$$

$$\rho_o \left[\frac{\partial u_t}{\partial t} + (u_t \cdot \nabla) u_o + (u_o \cdot \nabla) u_t \right] + \rho_t (u_o \cdot \nabla) u_o = \nabla \cdot \sigma + F - u_o M \tag{7}$$

$$\begin{aligned} \rho_o C_p \left[\frac{\partial T_t}{\partial t} + (u_t \cdot \nabla) T_o + (u_o \cdot \nabla) T_t \right] + \rho C_p (u_o \cdot \nabla) T_o - \alpha_p T_o \left[\frac{\partial p_t}{\partial t} + (u_t \cdot \nabla) p_o + (u_o \cdot \nabla) p_t \right] - \alpha_p T_t (u_o \cdot \nabla) p_o \\ = \nabla \cdot (k \nabla T_t) + \phi + Q \end{aligned} \tag{8}$$

where, ρ is the density, u is the velocity, T is the temperature, σ is the stress tensor, ϕ is the viscous dissipation function, M is the mass source, F is the volume force source, and Q is the heat source, C_p is the specific heat at constant pressure, and α_p is the coefficient of thermal expansion. The variables with a subscript t are the acoustic perturbation values and those with subscript o are the background mean flow values.

The TL of the muffler is subsequently determined by using the expression [21]:

$$TL = 20 \log \left\{ \left(\frac{A_i}{A_o} \right)^{1/2} \left(\frac{1 + M_i}{1 + M_o} \right) \left(\frac{Z_i}{Z_o} \right)^{1/2} \left| \frac{p_i^+}{p_o^+} \right| \right\} \tag{9}$$

where, the subscripts i and o denote the inlet and outlet tubes, respectively, A is the cross-sectional area, M is the Mach number, Z is the characteristic acoustic impedance of the medium and p^+ denotes the incident acoustic pressure wave which is the function of frequency.

3.2. Setup and analysis

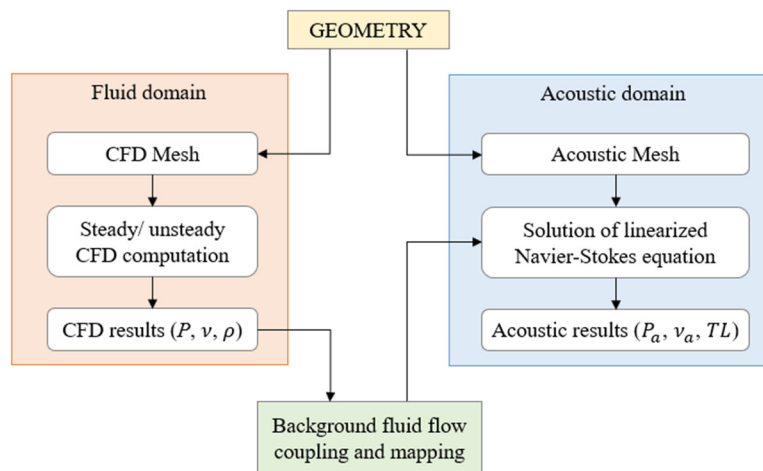


Fig. 6 Aeroacoustics analysis in COMSOL

A commercial software COMSOL is used to perform CFD [20] and acoustic analysis [22]. The methodology employed in this study consists of the following steps:

- (1) The shear-stress transport (SST) turbulence model is used to analyze the background flow in the muffler across different Mach numbers.
- (2) Subsequently, the acoustic problem is resolved through the application of the linearized Navier-Stokes physics interface.
- (3) The mean flow velocity, pressure, and turbulent viscosity are integrated with the LNSE model through the background fluid flow coupling Multiphysics feature.
- (4) A mapping technique is employed to transfer the flow solution from the CFD mesh to the acoustic mesh.
- (5) Pressure acoustics in the frequency domain are employed to address the no-flow scenario.

To further the understandable description of the aforementioned steps, a flow chart is presented in Fig. 6.

Regarding 3-D CFD analysis and subsequently the acoustic analysis, a tuned muffler (i.e., muffler with end correction applied) is considered. To save upon the computational cost, only one-half of the fluid domain of the muffler (maintaining its symmetry) is adopted for the analysis, as shown in Fig. 7. This fluid model of the muffler is further split into several parts for smooth meshing operation. The critical part of this analysis is the discretization or meshing process. The two meshed models used for CFD and acoustic analyses are shown in Fig. 8. The mesh model consists of hexahedral and tetrahedral elements with CFD mesh being denser (higher number of nodes), compared to the acoustic mesh model. A boundary layer mesh is used to capture no-slip conditions at the domain boundaries. In the case of acoustic mesh, although the mesh is a coarse mesh, compared to CFD, the size of the element is observed within the limit of 6 elements per wavelength at the highest frequency of interest (1600 Hz). To mimic an anechoic termination, a perfectly matched layer (PML) domain is created at the ends of the pipe.

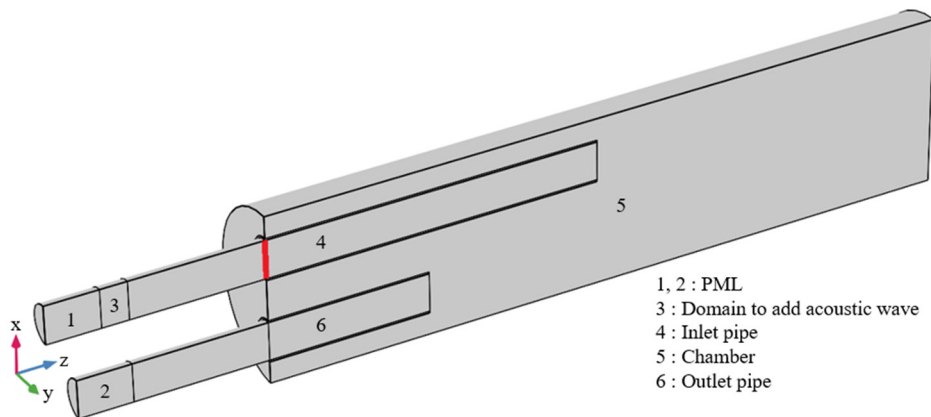


Fig. 7 One-half of the muffler model

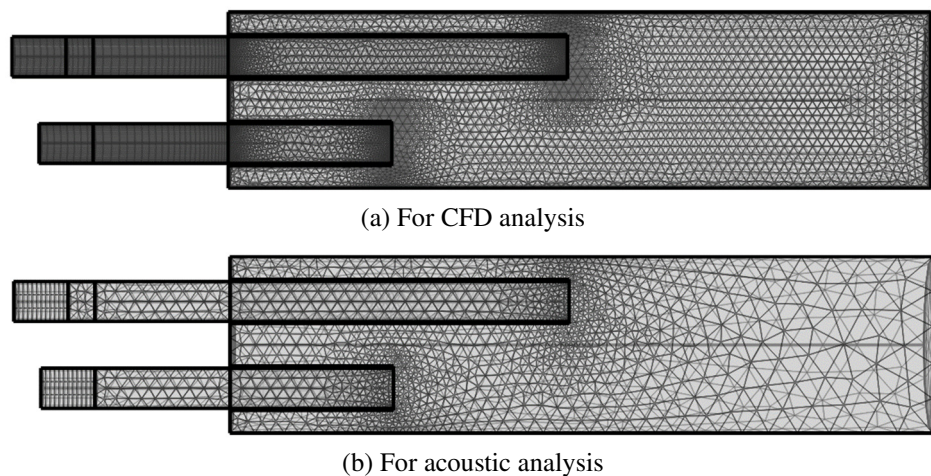


Fig. 8 Mesh model of SEIO muffler

The fluid domain is filled with air and is set as a compressible flow for $M < 0.3$, which is to consider spatially varying density in the exhaust mufflers which encounters a low Mach number of $M < 0.2$. The inlet is subjected to a fully developed turbulent flow of Magnitude $U_{in} = C_o M$, where $M = 0$ (no flow condition), 0.05, and 0.1, for temperature $T = 293$ K, 733 K, and 953 K. The turbulent flow, Menter SST interface is used, as this interface is capable of solving this single phase, compressible, low Mach number problem.

Upon solving the CFD model using the above conditions, the solution of this study is mapped onto the acoustic mesh using the built-in background fluid flow coupling Multiphysics feature and the dedicated mapping study, which is available in the COMSOL. To check the effectiveness of mapping, the axial flow velocity and the turbulent viscosity, which are evaluated on the CFD mesh compared with that of the mapped values on the acoustics mesh at one of the edges on the inlet pipe (edge marked in red color on inlet pipe in Fig. 7). This comparison is shown in Fig. 9 and Fig. 10 for $M = 0.05$ and 0.1.

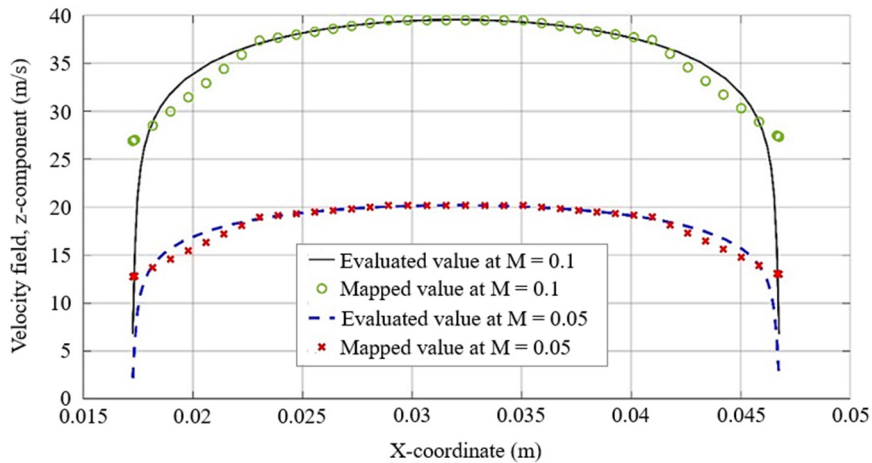


Fig. 9 Evaluated vs Mapped values of the Velocity field

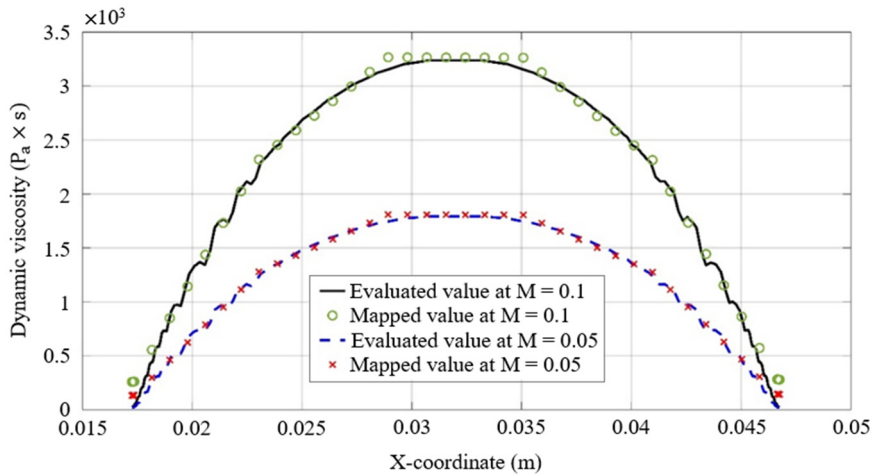


Fig. 10 Evaluated vs Mapped values of Dynamic Viscosity

The mapped values are satisfactory for solving the pressure acoustic problem and determining the TL in the frequency domain. The problem is first addressed for the no-flow scenario ($M = 0$), followed by all subsequent Mach numbers. Such a procedure is further repeated for all the temperature values in this study.

4. Results and Discussion

Using the 3-D CFD approach, the TL has been predicted in the tunned SEIO muffler in the presence of flow. Initially, the flow velocity, turbulent kinetic energy, and pressure distribution results are ascertained to interpret the flow behavior inside the muffler. Subsequently, the effect of this flow on the TL is examined scrupulously at different temperatures and Mach numbers to evaluate the acoustic attenuation properties of the muffler.

4.1. CFD results

The velocity distribution contour for $M = 0.05$ and 0.1 at 293 K is shown in Fig. 11. When the air flows through the inlet pipe inside the chamber, the velocity decreases due to an increase in the cross-sectional area. Furthermore, due to this sudden expansion, eddies are formed in the chamber, as shown in Fig. 12. However, as the flow reaches the outlet pipe, given the reduction in cross-sectional area, the flow is streamlined with an increase in the flow velocity. This increase in flow velocity may result in the aeroacoustics noise generation. A tendency, likewise, is observable as the temperature of the fluid is increased. The plot of pressure distribution, along the inlet and outlet pipes and in the chamber, is illustrated in Fig. 13. It is evident from the figure that the pressure decreases from the inlet pipe to the chamber and further into the outlet pipe. The net pressure loss in the muffler (i.e., the difference in pressure at the inlet and outlet pipe) is 2000 Pa , which is seemingly nominal.

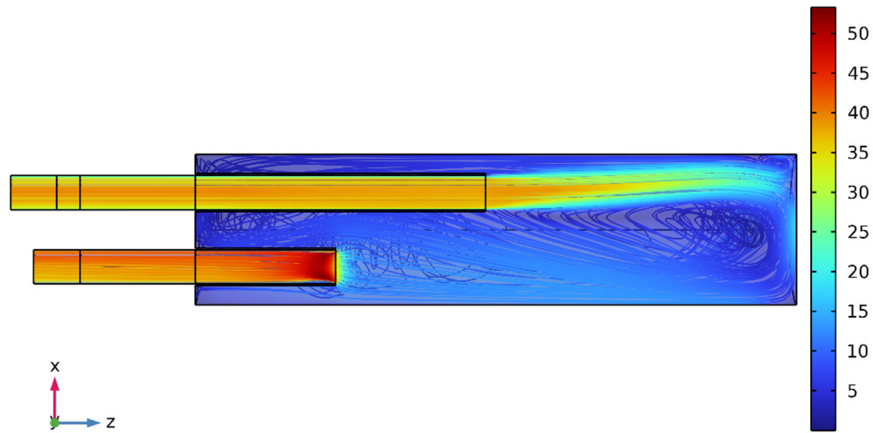


Fig. 11 Contour of flow velocity in (m/s) for $M = 0.1$

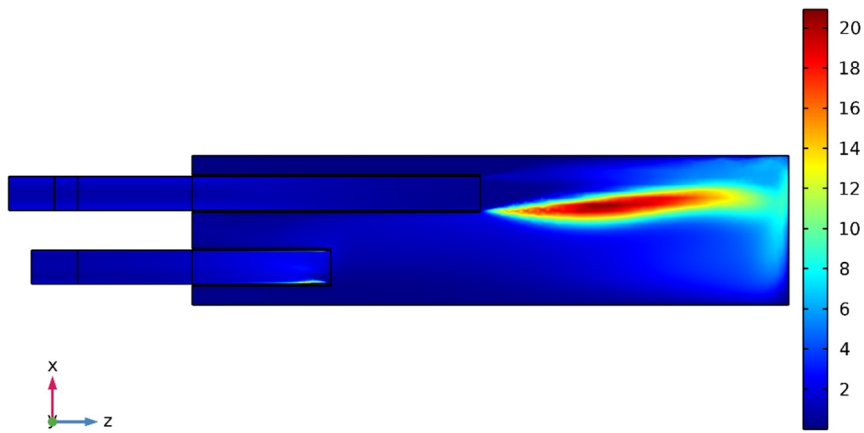


Fig. 12 Contour of turbulent kinetic energy (J/Kg) for $M = 0.1$

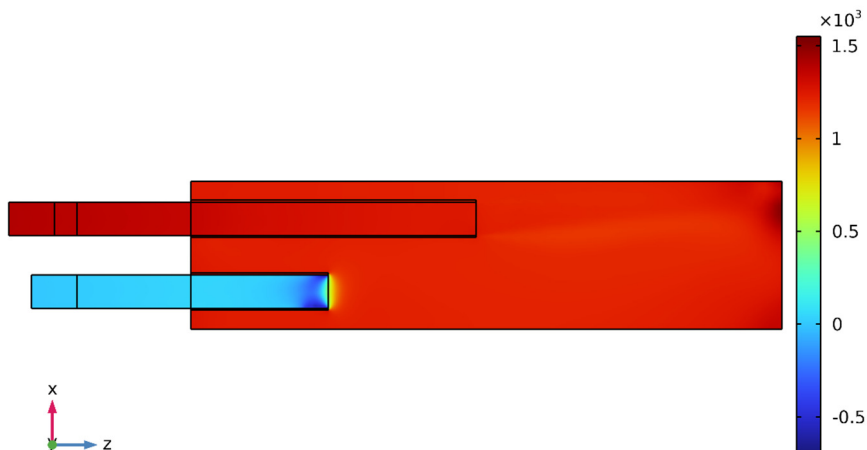
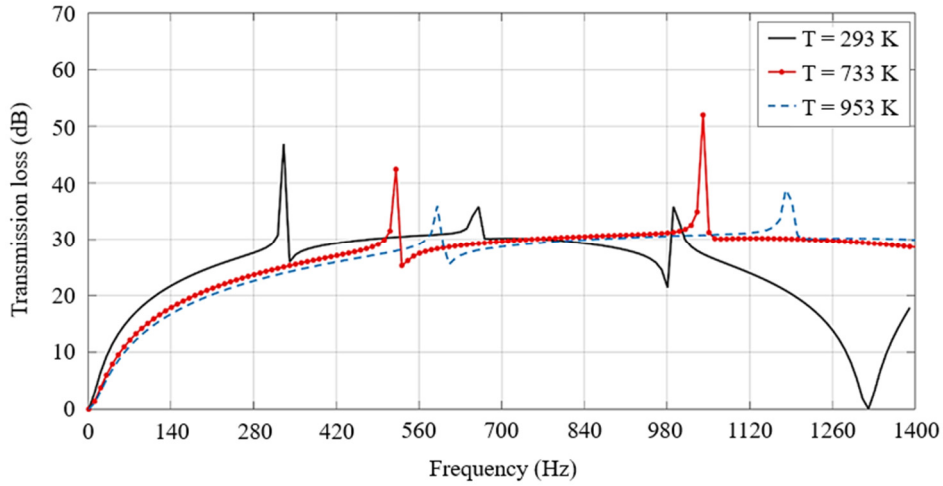


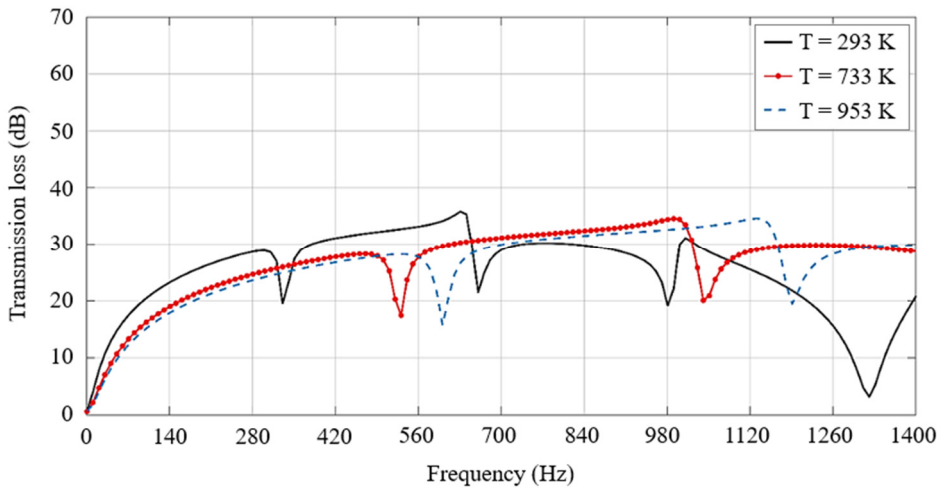
Fig. 13 Contour of pressure distribution (Pa) for $M = 0.1$

4.2. Effect of temperature and mean flow on the double tuning of the muffler

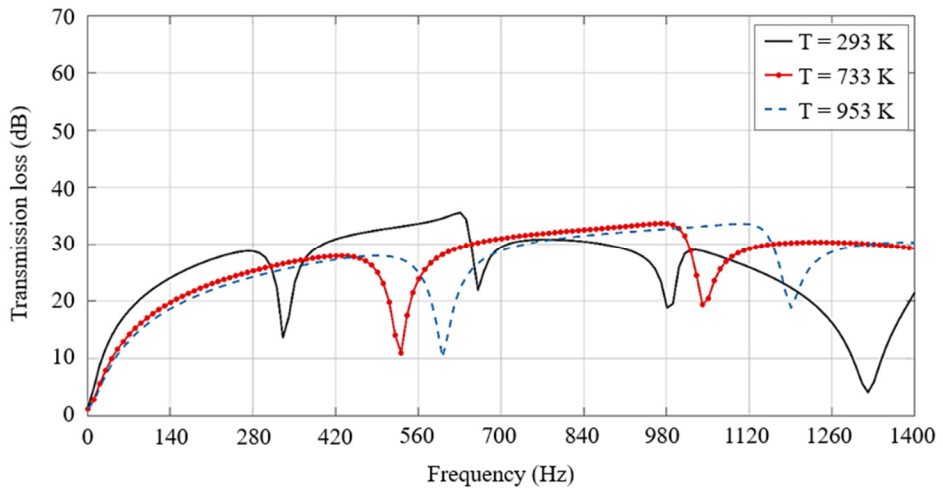
When three of the first four troughs in the TL plot are lifted pertinent to the corresponding SEC muffler, to yield a wide band TL, the muffler can be called a double-tuned muffler [23-24]. As shown in Fig. 2, the double tuning of the SEIO muffler in the absence of mean flow ($M = 0$) at room temperature (273 K) consequently increases the height of the TL dome by about 10 dB. The same double-tuned muffler has also retained its double tuning when tested with higher temperatures $T = 733$ K and 953 K with the mean flow for $M = 0.05$ and 0.1, as observed in Fig. 14.



(a) $M = 0$



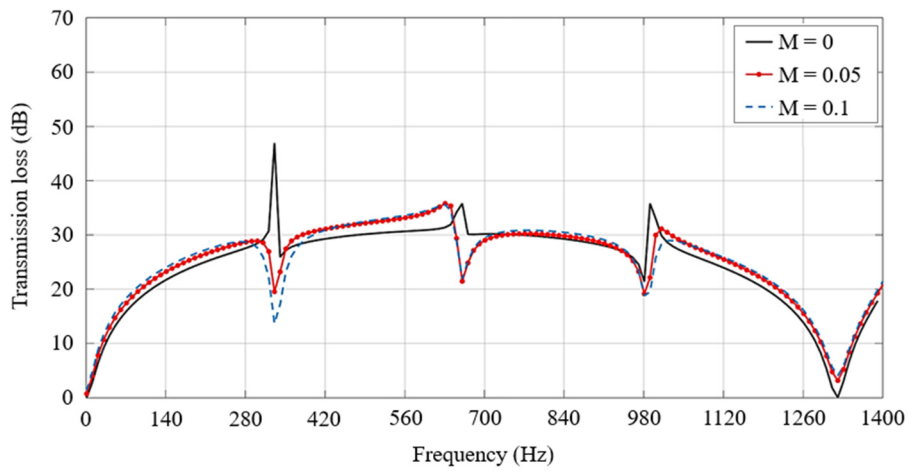
(b) $M = 0.05$



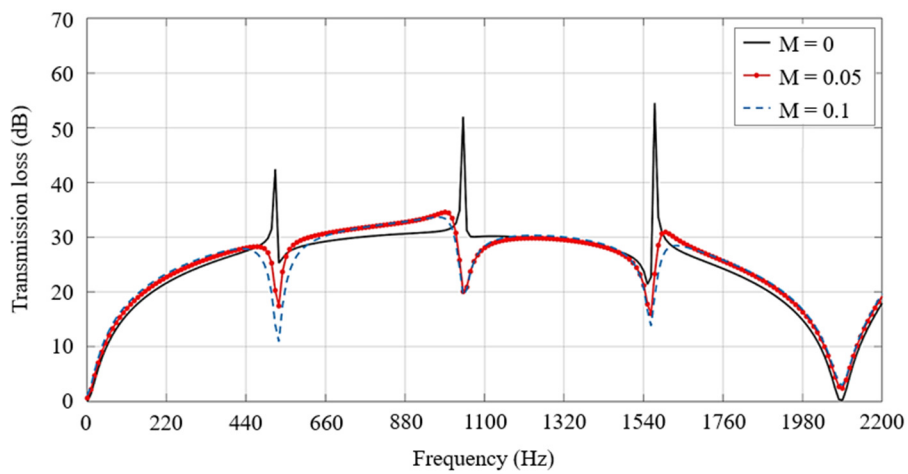
(c) $M = 0.1$

Fig. 14 Comparison of TL at different temperatures

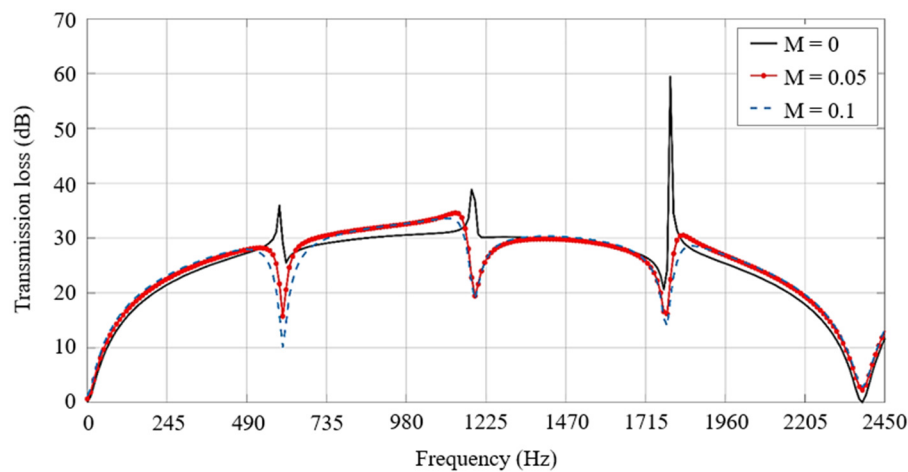
Specifically, the temperature correlates with speed of sound, thereby resulting in a significantly wider band TL plot, as shown in Fig. 14(a). In other words, the through of the TL plot for $T = 293\text{ K}$ is at 1321 Hz , whereas, at $T = 733\text{ K}$, it changes to approximately 2091 Hz . Additionally, at $T = 953\text{ K}$, it shifts even further to around 2381 Hz , which can be advantageous in some applications that demand a wider band TL. However, the TL curve is dropped in the lower frequency region, particularly in the absence of flow. Fortunately, the conditions are significantly better at a higher Mach number ($M = 0.1$), which will be the actual working condition of this muffler. Moreover, as shown in Fig. 14(b) and 14(c), a similar tendency is observed even at higher Mach numbers, i.e., at $M = 0.05$ and $M = 0.1$, wherein the TL plot results in a wider band, with a sharp dip in peaks due to the presence of flow.



(a) $T = 293\text{ K}$



(b) $T = 733\text{ K}$



(c) $T = 953\text{ K}$

Fig. 15 Comparison of TL for different Mach numbers

Furthermore, despite the effect of bias flow, the muffler retains its double tuning. Fig. 15(a) shows a substantial drop in the peak with increasing Mach number, which will degrade the acoustic performance of the muffler to some extent. Similarly, a tendency is observed by Ramya and Munjal [3] in their work of double tuning of the extended concentric tube resonator, wherein presents a mean flow with a considerable weakening of resonance peaks, resulting in sharp dips.

In the work of Sagar and Munjal [25], where they investigated the effect of mean flow at the H-junction of the fork muffler, which comprises a three-pass double-reversal muffler with a tubular bridge, even they observed that the magnitudes of the peaks are substantially diminished due to the mean flow effect at the junction. While investigating the effect of flow on the Helmholtz resonator, Selamet et al. [26] found that the introduction of mean flow intensely weakens the interaction between the cavity and the main duct, incurring the reduction of peak TL along with the shift in resonance frequency to higher values.

An increase in the mean flow increases the acoustic resistance and reactance thereby creating aeroacoustic damping, leading to a decrease in TL at the resonance peaks (as seen in Fig. 15). However, other than at the regions of sharp peaks, the TL curve is uplifted by marginal values as the flow velocity or Mach number increases, which can be factually inferred at higher temperatures, as shown in Fig. 15(b) and 15(c). Such a finding is undeniably advantageous, at least in the region of the lower frequency range [22]. Moreover, the previously seen adverse effect of higher temperatures in the lower frequency region can be perceived to be marginalized against the higher Mach number in Fig. 15(c).

5. Conclusions

The previously derived expressions to predict the end corrections of the inlet and outlet pipes have been experimentally verified. The derived expressions aptly manage to double-tune the muffler in the stationary medium. Furthermore, using three-dimensional CFD, the effect of mean flow and temperature on the double tuning of the flow reversal muffler has been effectively examined. The background fluid flow coupling of COMSOL software and mapping technique are efficient tools for considering the output of CFD analysis as an input to frequency domain acoustic analysis. The following section signifies important findings in this study:

- (1) The developed SEIO muffler performs admirably in the stationary medium. If a few deviations at certain frequencies (mainly due to fabrication errors) are ignored, the measured plot will mostly overlap with the predicted plot, which corroborates the validity of the end correction expression.
- (2) With higher Mach numbers, the flow velocity increases at the intersection of the chamber and outlet pipe, which may lead to generating aero-acoustic noise.
- (3) With the increase in temperature, the double tuning of the muffler is retained with a wider TL band, whereas with a compromise on the TL level in the lower frequency region.
- (4) Double tuning of the muffler is also retained when the mean flow is introduced, with a dip in the sharp peaks, nevertheless. However, the TL levels at other frequencies get uplifted thereby marginalizing the adverse effect of temperature at lower frequencies.

Acknowledgment

A sincere thanks to Dr. M. L. Munjal, Professor (Emeritus), FRITA, Department of Mechanical Engineering, IISc, Bengaluru, India for giving the original problem statement of the SEIO muffler. Also, a sincere thanks to Dr. K. M. Kumar, Assistant Professor, Department of Mechanical Engineering, IIT-Indore, India, for providing a computational facility to carry out this work.

Conflicts of Interest

The authors declare no conflict of interest.

References

- [1] M. L. Munjal, *Acoustics of Ducts and Mufflers*, 2nd ed., Hoboken: Wiley, 2014.
- [2] P. Chaitanya and M. Munjal, "Tuning of the Extended Concentric Tube Resonators," Indian Institute of Science, SAE Technical Paper 2011-26-0070, January 19, 2011.
- [3] E. Ramya and M. L. Munjal, "Improved Tuning of the Extended Concentric Tube Resonator for Wide-Band Transmission Loss," *Noise Control Engineering Journal*, vol. 62, no. 4, pp. 252-263, July 2014.
- [4] P. Chaitanya and M. L. Munjal, "Effect of Wall Thickness on the End Corrections of the Extended Inlet and Outlet of a Double-Tuned Expansion Chamber," *Applied Acoustics*, vol. 72, no. 1, pp. 65-70, January 2011.
- [5] C. D. Gaonkar, D. R. Rao, K. M. Kumar, and M. L. Munjal, "End Corrections for Double-Tuning of the Same-End Inlet-Outlet Muffler," *Applied Acoustics*, vol. 159, article no. 107116, February 2020.
- [6] C. I. J. Young and M. J. Crocker, "Acoustical Analysis, Testing, and Design of Flow-Reversing Muffler Chambers," *The Journal of the Acoustical Society of America*, vol. 60, no. 5, pp. 1111-1118, November 1976.
- [7] J. G. Ih and B. H. Lee, "Theoretical Prediction of the Transmission Loss of Circular Reversing Chamber Mufflers," *Journal of Sound and Vibration*, vol. 112, no. 2, pp. 261-272, January 1987.
- [8] A. Selamet and Z. L. Ji, "Acoustic Attenuation Performance of Circular Flow-Reversing Chambers," *The Journal of the Acoustical Society of America*, vol. 104, no. 5, pp. 2867-2877, November 1998.
- [9] A. Mimani and M. L. Munjal, "Acoustic End-Correction in a Flow-Reversal End Chamber Muffler: A Semi-Analytical Approach," *Journal of Computational Acoustics*, vol. 24, no. 02, article no. 1650004, June 2016.
- [10] V. B. Panicker and M. L. Munjal, "Aeroacoustics Analysis of Mufflers With Flow Reversals," *Journal of the Indian Institute of Science*, vol. 63, no. 1, pp. 21-38, January 1981.
- [11] A. Broatch, X. Margot, A. Gil, and F. D. Denia, "A CFD Approach to the Computation of the Acoustic Response of Exhaust Mufflers," *Journal of Computational Acoustics*, vol. 13, no. 02, pp. 301-316, June 2005.
- [12] H. Zhang, W. Fan, and L. X. Guo, "A CFD Results-Based Approach to Investigating Acoustic Attenuation Performance and Pressure Loss of Car Perforated Tube Silencers," *Applied Sciences*, vol. 8, no. 4, article no. 545, April 2018.
- [13] H. Huang, Z. Chen, and Z. Ji, "One-Way Fluid-to-Acoustic Coupling Approach for Acoustic Attenuation Predictions of Perforated Silencers With Non-Uniform Flow," *Advances in Mechanical Engineering*, vol. 11, no. 5, article no. 1687814019847066, May 2019.
- [14] L. Liu, X. Zheng, Z. Hao, and Y. Qiu, "A Time-Domain Simulation Method to Predict Insertion Loss of a Dissipative Muffler With Exhaust Flow," *Physics of Fluids*, vol. 33, no. 6, article no. 067114, June 2021.
- [15] Z. He, Z. Ji, and H. Huang, "Acoustic Attenuation Prediction of Perforated Reactive and Dissipative Mufflers With Flow by Using Frequency-Domain Linearized Navier-Stokes Equations," *International Journal of Acoustics & Vibration*, vol. 28, no. 4, pp. 394-402, December 2023.
- [16] H. Zhirong, J. Zhenlin, and F. Yiliang, "Acoustic Attenuation Prediction and Analysis of Perforated Hybrid Mufflers With Non-Uniform Flow Based on Frequency Domain Linearized Navier-Stokes Equations," *Advances in Mechanical Engineering*, vol. 16, no. 1, article no. 16878132231226055, January 2024.
- [17] B. Mohamad, J. Karoly, A. Zelentsov, and S. Amroune, "Investigation of Perforated Tube Configuration Effect on the Performance of Exhaust Mufflers With Mean Flow Based on Three-Dimensional Analysis," *Archives of Acoustics*, vol. 46, no. 3, pp. 561-566, 2021.
- [18] M. Bugaru and C. M. Vasile, "Recent Developments in Using a Modified Transfer Matrix Method for an Automotive Exhaust Muffler Design Based on Computation Fluid Dynamics in 3D," *Computation*, vol. 12, no. 4, article no. 73, April 2024.
- [19] D. P. Jena and S. N. Panigrahi, "Numerically Estimating Acoustic Transmission Loss of a Reactive Muffler With and Without Mean Flow," *Measurement*, vol. 109, pp. 168-186, October 2017.
- [20] COMSOL, "The CFD Module User's Guide," <https://doc.comsol.com/6.2/doc/com.comsol.help.cfd/CFDModuleUsersGuide.pdf>, December 14, 2023.
- [21] Z. He, Z. Ji, and H. Huang, "Acoustic Attenuation Analysis of Expansion Chamber Mufflers With Non-Uniform Cold and Hot Flow," *Journal of Sound and Vibration*, vol. 568, article no. 118062, January 2024.

- [22] COMSOL, "The Acoustics Module User's Guide," <https://doc.comsol.com/5.4/doc/com.comsol.help.aco/AcousticsModuleUsersGuide.pdf>, December 14, 2023.
- [23] K. M. Kumar, C. D. Gaonkar, and M. L. Munjal, "Double-Tuning and Experimental Validation of Rotated-Offset Inlet-Outlet Circular Chamber Muffler," *Applied Acoustics*, vol. 197, article no. 108948, August 2022.
- [24] C. D. Gaonkar and M. L. Munjal, "Theory of the Double-Tuned Side-Inlet Side-Outlet Muffler," *Noise Control Engineering Journal*, vol. 66, no. 6, pp. 489-495, December 2018.
- [25] V. Sagar and M. L. Munjal, "Analysis and Design Guidelines for Fork Muffler With H-Connection," *Applied Acoustics*, vol. 125, pp. 49-58, October 2017.
- [26] E. Selamet, A. Selamet, A. Iqbal, and H. Kim, "Effect of Flow on Helmholtz Resonator Acoustics: A Three-Dimensional Computational Study vs. Experiments," The Ohio State University, SAE Technical Paper 2011-01-1521, May 17, 2011.



Copyright© by the authors. Licensee TAETI, Taiwan. This article is an open-access article distributed under the terms and conditions of the Creative Commons Attribution (CC BY-NC) license (<https://creativecommons.org/licenses/by-nc/4.0/>).